

Exact versus mean-field solutions in a rotating Bose-Einstein condensate

G. M. Kavoulakis¹, B. Mottelson², and S. M. Reimann¹

¹*Mathematical Physics, Lund Institute of Technology, P.O. Box 118, S-22100 Lund, Sweden*

²*NORDITA, Blegdamsvej 17, DK-2100 Copenhagen Ø, Denmark*

(December 2, 2024)

We examine the equivalence between “exact” and mean-field solutions for the lowest state of a harmonically-trapped, weakly-interacting Bose-Einstein condensate of atoms which rotates with a given angular momentum. Making use of the pair correlation function, we demonstrate that the solutions from the two approaches give essentially the same results in the asymptotic limit of a large number of atoms in the trap.

PACS numbers: 03.75.Fi, 05.30.Jp, 67.40.Db, 67.40.Vs

I. INTRODUCTION

A gas of Bose-Einstein condensed atoms confined in a harmonic potential provides an ideal system for studying phenomena connected with long-range order, superfluidity, quantized vortex states, etc. Recent experiments in vapors of trapped alkali-metal atoms [1–4] involving rotation were performed in the Thomas-Fermi regime of strong interactions between the atoms and observed an array of vortices as the angular momentum per particle increased, confirming that the physics in this limit is similar to that of liquid ⁴He. Moreover, in the experiment of Abo-Shaeer *et al.* [3], where more than 100 vortices were observed, one could reach the limit of weak interactions between the atoms, as pointed out by Ho [5]. In a weakly interacting gas, the coherence length is larger than the size of the cloud, as in paired atomic nuclei under rotation.

The problem of a harmonically trapped, weakly-interacting Bose-Einstein condensate under rotation has been studied theoretically by several authors [6–12]. Both the mean field approximation using the Gross-Pitaevskii equation [7,10] and “exact” numerical diagonalization approaches [6,9] were considered.

As shown in Ref. [11], the interaction energy calculated within the mean-field approximation emerges as the correct leading-order approximation to exact calculations in a given subspace. In the present study we provide further evidence that the two methods give the same results in the asymptotic limit. Our study is based on the pair correlation function [13,12], where one essentially fixes the position of one atom on a “reference point”, calculating the probability of locating an atom at a different point. Using this method, Liu *et al.* [12] recently questioned the mean-field mechanism for the emergence of vortices with increasing L and stated that the single and double vortex states are generated at the center of the cloud. This is in apparent contradiction to the Gross-Pitaevskii approach, which predicts that the vortices successively enter the cloud from its outer parts as L/N (where N is the number of atoms in the trap and $\hbar L$ is the angular momentum of the system) increases [7,10]. Our

analysis, however, confirms the validity of the mean-field approach: the pair correlations are found to be consistent with the vortices entering from the periphery of the cloud.

II. THE MODEL

Let us start with the model we consider. Our Hamiltonian is $H = \sum_i h_i + V$, where

$$h_i = -\frac{\hbar^2}{2M} \nabla_i^2 + \frac{1}{2} M \omega^2 r_i^2 \quad (1)$$

includes the kinetic energy of the particles and the potential energy due to the trap, and

$$V = \frac{1}{2} U_0 \sum_{i \neq j} \delta(\mathbf{r}_i - \mathbf{r}_j) \quad (2)$$

is the two-body interaction between particles, which is assumed to be of zero range. Here M is the atomic mass, ω is the frequency of an isotropic trapping potential, and $U_0 = 4\pi\hbar^2 a/M$ is the strength of the effective two-body interaction, with a being the scattering length for atom-atom collisions. We assume that $a > 0$, i.e., we treat only the case of repulsive effective interactions between the atoms. The restriction of weak interactions requires that

$$nU_0 \ll \hbar\omega, \quad (3)$$

where n is the density of the atoms at the center of the trap. As we are interested in the lowest-energy states as a function of the total angular momentum (the so-called “yrast line”) we can work in a subspace of harmonic oscillator states with radial quantum number $n_r = 0$ and single-particle angular momentum $0 \leq m \leq L$ [8]. In the absence of interactions, these states are degenerate.

Let us now briefly describe the two methods which have been used to study the yrast line, starting with the mean-field approach [7,10]. Within this approximation the many-body wavefunction $\Psi_{L,N}(\mathbf{r}_1, \mathbf{r}_2, \dots, \mathbf{r}_N)$

with N particles and L units of angular momentum is a Fock state expressed as a simple product of single-particle states:

$$\Psi_{L,N}(\mathbf{r}_1, \mathbf{r}_2, \dots, \mathbf{r}_N) = \psi(\mathbf{r}_1) \times \psi(\mathbf{r}_2) \dots \psi(\mathbf{r}_N). \quad (4)$$

It is natural to expand the single-particle states $\psi(\mathbf{r}_i)$ in the basis of the harmonic-oscillator eigenstates $\phi_m(\mathbf{r}_i)$ with angular momentum $m\hbar$ along the axis of rotation:

$$\psi(\mathbf{r}_i) = \sum_{m=0}^{\infty} c_m \phi_m(\mathbf{r}_i), \quad (5)$$

where c_m are variational parameters. Also

$$\phi_m(\mathbf{r}) = \frac{1}{(m!\pi^{3/2}a_0^3)^{1/2}} \left(\frac{\rho}{a_0}\right)^{|m|} e^{im\phi} e^{-(\rho^2+z^2)/2a_0^2}, \quad (6)$$

where ρ, z , and ϕ are cylindrical polar coordinates, and a_0 is the oscillator length given by $(\hbar/M\omega)^{1/2}$. In Eq. (6) the gas is assumed to be in its ground state for motion along the axis of rotation, i.e., the z -axis. The quantity $|c_m|^2$ gives the probability for the occupancy of state ϕ_m . One imposes two constraints on the parameters c_m . The wavefunction must be normalized, $\sum_m |c_m|^2 = 1$, and the expectation value of the angular momentum per atom must be fixed, $\sum_m m|c_m|^2 = L/N$. The expectation value of the interaction energy V in the state given by Eq. (4) is

$$\langle V \rangle = \frac{1}{2}N(N-1)U_0 \int |\psi(\mathbf{r})|^4 d\mathbf{r}. \quad (7)$$

Minimizing $\langle V \rangle$ with respect to the c_m subject to the two constraints given above, one obtains the mean field energy and the corresponding wavefunction.

Let us now turn to the exact diagonalization method [6,9]. Being interested only in the yrast spectrum, the above mentioned restriction $n_r = 0$ and $0 \leq m \leq L$ of the single-particle basis set allows us to work in a finite-dimensional subspace, spanned by the states $|\mathcal{L}\rangle = |N_0, N_1, N_2, \dots, N_L\rangle$ where N_m is the number of atoms in the state ϕ_m , Eq. 6. These are eigenstates of the number operator, $\sum_m N_m = N$ and of the angular momentum, $\hbar \sum_m m N_m = \hbar L$. The interaction energy is given by

$$\hat{V} = \frac{1}{2}U_0 \sum_{i,j,k,l} I_{i,j,k,l} a_i^\dagger a_j^\dagger a_k a_l \quad (8)$$

with the boson creation and annihilation operators a_k^\dagger and a_k , and the two-body matrix elements [9]

$$I_{i,j,k,l} = \delta_{i+j,k+l} \frac{(i+j)!}{2^{(i+j)} \sqrt{i!j!k!l!}} \int d\mathbf{r} |\phi_0(\mathbf{r})|^4. \quad (9)$$

Diagonalizing the matrix $\langle \mathcal{L} | \hat{V} | \mathcal{L}' \rangle$ one obtains the eigenstates and eigenenergies of the system. As long as the limit of weak interactions is valid, this approach is exact. As for very large L and N the dimensionality of the subspace increases dramatically, this limit becomes numerically inaccessible. A further truncation of the basis to small m -values, however, offers a compromise which in many cases still yields the correct physical picture.

III. PAIR CORRELATION AND VORTEX FORMATION

The single-particle density of the atoms in some state Ψ is

$$n(\mathbf{r}) = \frac{1}{N} \langle \Psi | \sum_i \delta(\mathbf{r} - \mathbf{r}_i) | \Psi \rangle. \quad (10)$$

In the Fock state of Eq. (4), $n(\mathbf{r}) = |\psi(\mathbf{r})|^2$ is not in general axially symmetric. On the other hand, in the “exact” state $|\Psi_{L,N}\rangle$, $n(\mathbf{r})$ is axially symmetric as a result of the azimuthal symmetry of the Hamiltonian, Eq. 1.

In order to study the mechanism for the entry of vortices into the cloud, we therefore need to break this symmetry. This, for example, can be done by calculating the two-particle correlation between the density at a fixed point \mathbf{r}_A and a second point \mathbf{r} . The resulting function of \mathbf{r} will in general exhibit mirror symmetry with respect to the vector \mathbf{r}_A . More precisely we calculated the function

$$P(\mathbf{r}, \mathbf{r}_A) = \frac{\langle \Psi_{L,N} | \sum_{i \neq j} \delta(\mathbf{r} - \mathbf{r}_i) \delta(\mathbf{r}_A - \mathbf{r}_j) | \Psi_{L,N} \rangle}{(N-1) \langle \Psi_{L,N} | \sum_j \delta(\mathbf{r}_A - \mathbf{r}_j) | \Psi_{L,N} \rangle}. \quad (11)$$

It is worth pointing out that with the assumption of the mean-field many-body wavefunction of Eq. (4) (having a simple product form), $P(\mathbf{r}, \mathbf{r}_A)$ is proportional to the single-particle density, $P(\mathbf{r}, \mathbf{r}_A) = N^2 n(\mathbf{r}) = N^2 |\psi(\mathbf{r})|^2$ and is independent of the reference point \mathbf{r}_A . Using the exact wavefunction, however, this is not the case, as shown below.

Figures 1 and 2 show equidensity lines of $P(\mathbf{r}, \mathbf{r}_A)$, Eq. (11), calculated within the exact numerical diagonalization of the Hamiltonian for different values of N and L . In these figures we chose $\mathbf{r}_A = (x, y) = (3, 0)$ in units of the oscillator length a_0 . The blue colour denotes regions of lower density, while the red colour denotes regions of higher density.

More specifically, in Fig. 1 we have taken $N = 40$ particles and $L = 28, 32, 36$, and 40 , i.e., $L/N = 0.7, 0.8, 0.9$, and 1.0 . We have also used the same basis truncation as in Ref. [10] by considering the states with $0 \leq m \leq 6$ (the states with $m > 6$ do not affect the present calculation appreciably, since their occupancy for the range of values of L/N considered is very low [10].) Figure 1 with $L/N = 1$ corresponds to a single-vortex-like state and is slightly asymmetric with respect to the center because of the finite number of atoms we have considered. We have confirmed numerically that this asymmetry disappears as N gets larger. Figure 2 shows $P(\mathbf{r}, \mathbf{r}_A)$ for $L = 62, 64, 72$, and 84 , i.e., for $L/N = 1.55, 1.6, 1.8$, and 2.1 .

Figures 1 and 2 show a close resemblance with the ones given by the mean-field approximation [7,10]. We observe, for example, that the vortices enter the cloud from its outer parts, and also that an array of vortices develops as L/N increases. In addition there is an abrupt transition from a state with a nearly two-fold symmetry to an approximately three-fold symmetric state for $L/N \approx 2$,

in agreement with mean-field theory [10]. (We note that the deviations from a strictly two- or threefold symmetry are due to finite- N effects.)

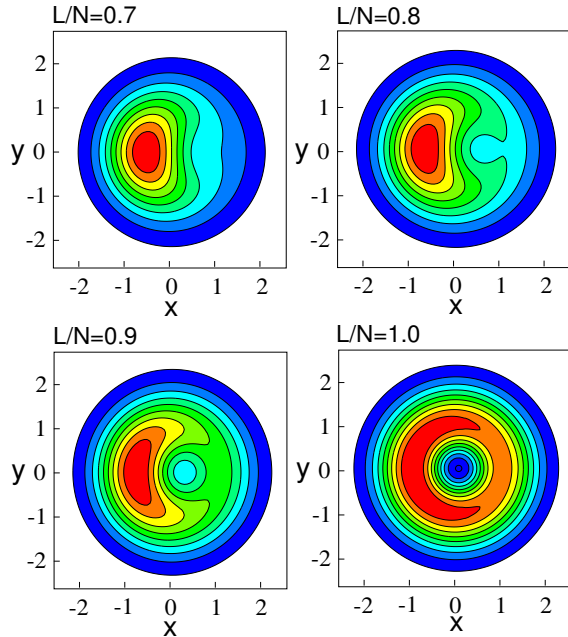


FIG. 1. Equidensity lines of $P(\mathbf{r}, \mathbf{r}_A)$ for $N = 40$ and $L = 28, 32, 36$, and 40 , calculated with the reference point located at $\mathbf{r}_A = (3, 0)$. Nine contours are shown, corresponding to decimal fractions of the maximum in the correlation function. The blue colour denotes regions of low density, while the red colour denotes regions of high density. The unit of length is the oscillator length a_0 . These pictures show how a vortex enters the bosonic cloud from its outer part.

As finite-size effects can lead to additional complications, when comparing the results of exact diagonalization to those of the mean-field approach, ideally we have to explore very large values of N and L . However, this is numerically impossible due to the rapid increase in the dimensionality of the subspace used. However, a carefully chosen truncation of the basis still allows us to consider fairly large values of N and L without any significant effect on the physical picture. We note that the correlation functions in general depend on the choice of the reference point. One needs to be careful how this point is chosen in order to get a useful physical picture. While we could confirm the results of Ref. [12] for the specific choice of the reference point that the authors made, we found that for a different choice of \mathbf{r}_A the picture changes: the orientation of the equidensity lines of the pair correlation function with respect to the vector \mathbf{r}_A in fact depends on its length (see Figs. 3 and 4). This observation leads to a disagreement with the conclusion of Ref. [12] that the vortices are generated at the center of the cloud, as can be seen clearly in Figs. 1 and 2, and we can demonstrate quantitatively the equivalence of the mean-field solutions with the exact approach (in the asymptotic limit).

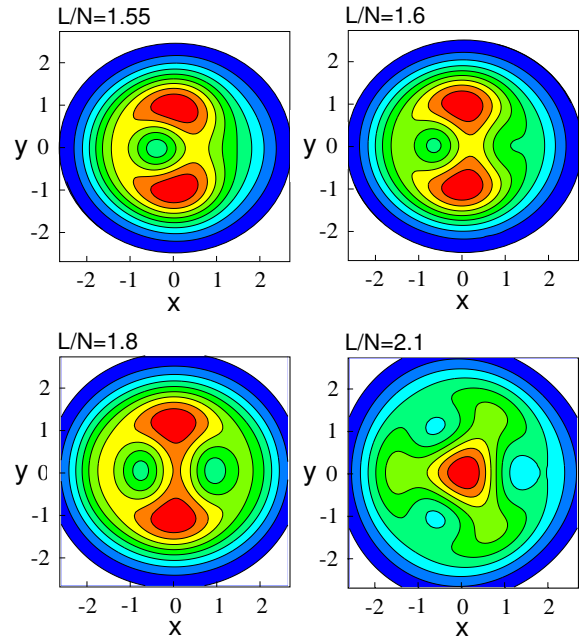


FIG. 2. Same as Fig. 1 for $N = 40$ and $L = 62, 64, 72$, and 84 . These pictures show how a second vortex enters the cloud, eventually leading to a nearly two-fold symmetric state ($L/N = 1.8$.) For higher values of L/N ($= 2.1$) a state with approximately three-fold symmetry forms. (The deviations from a strictly two- or threefold symmetry are due to finite- N effects.)

IV. A MORE QUANTITATIVE COMPARISON

A. Below the unit vortex

It is instructive to examine a specific example, so let us consider the case $L/N \lesssim 1$. As we move the reference point \mathbf{r}_A , when $L/N \lesssim 1$, the equidensity lines of the pair correlation function rotate by π , as shown in Fig. 3. This effect can be explained on the basis of the Gross-Pitaevskii approach: we know from the mean-field results [10], that for $L/N \lesssim 1$ the order parameter is dominated by the states with $m = 0, 1$ and 2 , and thus to leading order,

$$\psi(\mathbf{r}) = c_0 \phi_0(\mathbf{r}) + c_1 \phi_1(\mathbf{r}) + c_2 \phi_2(\mathbf{r}), \quad (12)$$

with

$$\begin{aligned} |c_0|^2 &= 2l, \\ |c_1|^2 &= 1 - 3l, \\ |c_2|^2 &= l, \end{aligned} \quad (13)$$

where $l = 1 - L/N$. The signs of c_0 and c_2 have to be opposite, in order to minimize the interaction energy [10]. One sees immediately from the above equation that for $L/N = 1$, the lowest state of the system is “single-vortex”

like, with only the state with $m = 1$ being macroscopically occupied. Equation (12) implies that for $L < N$, the single-particle density $n(\mathbf{r})$ takes the form (we assume for simplicity that $z = 0$)

$$n(\rho, \phi) = |\psi|^2 = f_0(\rho) + f_1(\rho) \cos(\phi), \quad (14)$$

where $f_m(\rho)$ are polynomials in ρ ,

$$f_1(\rho) \propto |c_0| - (\rho/a_0)^2 |c_2|/\sqrt{2}. \quad (15)$$

Under the transformation $\phi \rightarrow \phi + \pi$ the second term on the right side of Eq. (14) changes sign,

$$n(\rho, \phi + \pi) = f_0(\rho) - f_1(\rho) \cos(\phi). \quad (16)$$

By analogy to the mean-field approximation, the equidensity lines of the pair correlation function calculated within the exact diagonalization rotate by π at the values of ρ determined by the roots of the polynomial $f_1(\rho)$. According to Eq. (13), this root ρ_t is at $\rho_t/a_0 = \sqrt{2}$.

To confirm this, we diagonalized numerically the Hamiltonian, in the truncated space $m = 0, 1$ and 2 , since for $L/N \lesssim 1$ the many-body state is dominated by these three states [6,10]. This truncation allows us to consider much larger values of L and N and thus to get rid of small- N and L effects.

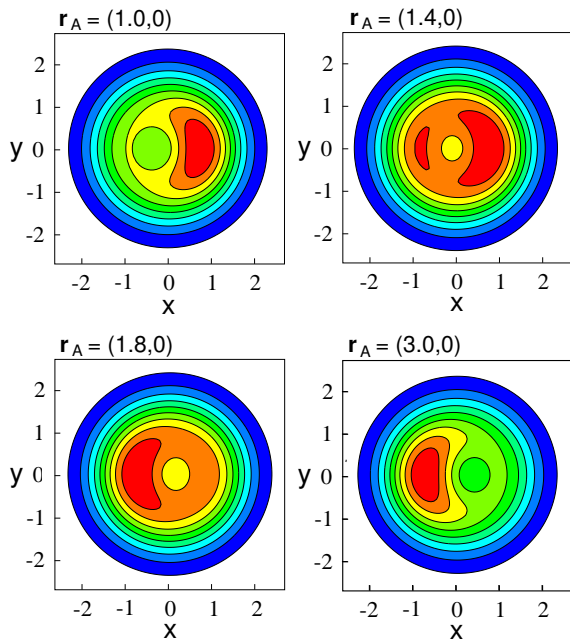


FIG. 3. Equidensity lines of $P(\mathbf{r}, \mathbf{r}_A)$ below the single vortex with $N = 800$ and $L = 640$ and $0 \leq m \leq 2$ for various positions of the reference point \mathbf{r}_A at $(1.0, 0)$, $(1.4, 0)$, $(1.8, 0)$, and $(3.0, 0)$. Between $(1.4, 0)$ and $(1.6, 0)$ (the latter not shown in the figure) the orientation of the correlation function rotates by π .

Figure 3 shows the pair correlations for $N = 800$ and $L = 640$, i.e., $L/N = 0.8$. The turning point of the equidensity lines is not sharply defined, but the transition occurs in the interval $1.4 < |\mathbf{r}_A| < 1.6$, in agreement with the number predicted by the mean-field approximation, $\rho_t/a_0 = \sqrt{2}$.

B. Below the double vortex

Completely similar arguments apply to the region $L/N \lesssim 2.0$. As we move the reference point \mathbf{r}_A towards the cloud periphery, when $L/N \lesssim 2$ the equidensity lines of the pair correlation function rotate by $\pi/2$ as shown in Fig. 4 (instead of π as in the case $L/N \lesssim 1$.) To see this, let us start from the mean-field approximation [7,10]. For $1.75 < L/N < 2.03$ only states with even indices are macroscopically occupied, $c_{2m+1} = 0$ [10]. Therefore the order parameter is given by

$$\psi(\mathbf{r}) = \sum_{m=0}^{\infty} c_{2m} \phi_{2m}(\mathbf{r}). \quad (17)$$

The corresponding single-particle density $n(\mathbf{r})$ is (at $z = 0$)

$$n(\rho, \phi) = |\psi|^2 = \sum_{m=0}^{\infty} f_{2m}(\rho) \cos(2m\phi). \quad (18)$$

One can include as many states as necessary, but we work with a toy model which captures the essential physics we want to demonstrate, including the states with $0 \leq m \leq 4$ (we comment below on the possibility of including more states.) Again this truncation allows us to consider much larger values of L and N in the numerical diagonalization, and thus to get rid of small- N and L effects, and also we get a simple and analytic answer. In this truncated basis we get

$$n(\rho, \phi) = f_0(\rho) + f_2(\rho) \cos(2\phi) + f_4(\rho) \cos(4\phi). \quad (19)$$

Under the transformation $\phi \rightarrow \phi + \pi/2$,

$$n(\rho, \phi + \pi/2) = f_0(\rho) - f_2(\rho) \cos(2\phi) + f_4(\rho) \cos(4\phi), \quad (20)$$

i.e., the sign of the second term changes, whereas the signs of the two other terms remain the same. Since

$$f_2(\rho) \propto |c_0| - (\rho/a_0)^4 |c_4|/\sqrt{24}, \quad (21)$$

and because $c_0 = -c_4$ at the minimum of the interaction energy [10]. We conclude that the “turning” point occurs in this case at $\rho_t/a_0 = 24^{1/8} \approx 1.488$. We found good agreement of this prediction of the mean-field approximation with the pair correlations, where, as shown in Fig. 4, $1.4 < |\mathbf{r}_A| < 1.6$.

Working in a more extended subspace of states, $m > 4$, one can see that the mean-field approximation predicts the existence of more turning points; however we have not been able to observe them. In the case $0 \leq m \leq 6$, for example, and for $L/N = 2$, according to the mean-field approximation there are two turning points, located at $\rho_t/a_0 \approx 1.49$ and ≈ 3.84 . We believe that we have not found the second turning point because of the small number of L and N we could consider numerically.

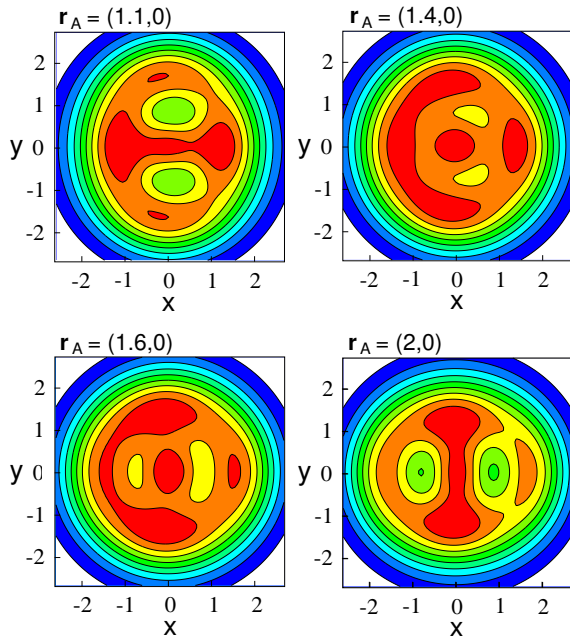


FIG. 4. Equidensity lines of $P(\mathbf{r}, \mathbf{r}_A)$ with $N = 50$ and $L = 100$ and $0 \leq m \leq 4$ for various positions of the reference point \mathbf{r}_A at $(1.1, 0)$, $(1.4, 0)$, $(1.6, 0)$, and $(2.0, 0)$. Between $(1.4, 0)$ and $(1.6, 0)$ one sees that the orientation of the correlation function rotates by $\pi/2$.

V. CONCLUSIONS

To summarize, we have examined the lowest state of a weakly-interacting Bose-Einstein condensate under rotation. We have demonstrated that in the asymptotic limit of large numbers of atoms and units of angular momentum, the “exact” solutions of this problem give equivalent results with the mean-field solutions. This result is consistent with Ref. [11], where it was shown that to leading order in N , the energy given by the two approaches is also the same. We have demonstrated that within the exact approach the vortices enter from the outer parts of the cloud, in agreement with the mean-field approach [7,10]. Finally we have examined a quantitative way of comparing these two approaches, which also demonstrates the equivalence of the two methods.

VI. ACKNOWLEDGEMENTS

We acknowledge inspiring discussions with A. D. Jackson, M. Koskinen, M. Manninen and D. Pfannkuche. Financial support was obtained by the “Bayerische Staatsministerium für Wissenschaft und Kultus”, NORDITA and the Swedish Research Council.

-
- [1] M. R. Matthews, B. P. Anderson, P. C. Haljan, D. S. Hall, C. E. Wieman, and E. A. Cornell, Phys. Rev. Lett. **83**, 2498 (1999).
 - [2] K. W. Madison, F. Chevy, W. Wohlleben, and J. Dalibard, Phys. Rev. Lett. **84**, 806 (2000); J. Mod. Opt. **47**, 2715 (2000).
 - [3] J. R. Abo-Shaeer, C. Raman, J. M. Vogels, and W. Ketterle, Science **292**, 476 (2001).
 - [4] E. Hodby, G. Hechenblaikner, S. A. Hopkins, O. M. Maragò, and C. J. Foot, e-print cond-mat/0106262.
 - [5] Tin-Lun Ho, Phys. Rev. Lett. **87**, 060403 (2001).
 - [6] N. K. Wilkin, J. M. F. Gunn, and R. A. Smith, Phys. Rev. Lett. **80**, 2265 (1998).
 - [7] D. A. Butts, and D. S. Rokhsar, Nature **397**, 327 (1999).
 - [8] B. Mottelson, Phys. Rev. Lett. **83**, 2695 (1999).
 - [9] G. F. Bertsch, and T. Papenbrock, Phys. Rev. Lett. **83**, 5412 (1999).
 - [10] G. M. Kavoulakis, B. Mottelson, and C. J. Pethick, Phys. Rev. A **62**, 63605 (2000).
 - [11] A. D. Jackson, G. M. Kavoulakis, B. Mottelson, and S. M. Reimann, Phys. Rev. Lett. **86**, 945 (2001).
 - [12] X. Liu, H. Hu, L. Chang, W. Zhang, S.-Q. Li, and Y.-Z. Wang, Phys. Rev. Lett. **87**, 030404 (2001).
 - [13] G. S. Ezra and R. S. Berry, Phys. Rev. A **28**, 1974 (1983).